European Journal of Pharmaceutical Sciences 74 (2015) 103–117

Contents lists available at ScienceDirect

European Journal of Pharmaceutical Sciences

journal homepage: www.elsevier.com/locate/ejps

An *in situ* gelling liquid crystalline system based on monoglycerides and polyethylenimine for local delivery of siRNAs

Lívia Neves Borgheti-Cardoso [a], Lívia Vieira Depieri [a], Sander A.A. Kooijmans [b], Henrique Diniz [a], Ricardo Alexandre Junqueira Calzzani [c], Fabiana Testa Moura de Carvalho Vicentini [a], Roy van der Meel [b], Márcia Carvalho de Abreu Fantini [d], Mamie Mizusaki Iyomasa [e], Raymond M. Schiffelers [b], Maria Vitória Lopes Badra Bentley [a,*]

[a] Faculdade de Ciências Farmacêuticas de Ribeirão Preto, Universidade de São Paulo, Av. do Café, s/n, 14040–903 Ribeirão Preto, SP, Brazil
[b] Laboratory of Clinical Chemistry and Haematology, University Medical Center Utrecht, Utrecht, The Netherlands
[c] Universidad de La Frontera, Avenida Francisco Salazar 01145, Temuco, Chile
[d] Instituto de Física, Universidade de São Paulo, São Paulo, SP, Brazil
[e] Faculdade de Odontologia de Ribeirão Preto, Universidade de São Paulo, Ribeirão Preto, SP, Brazil

ARTICLE INFO

Article history:
Received 17 December 2014
Received in revised form 16 April 2015
Accepted 20 April 2015
Available online 25 April 2015

Keywords:
Self-assembly
Non-viral gene delivery
siRNA
Local release
Liquid crystal

ABSTRACT

The development of delivery systems able to complex and release siRNA into the cytosol is essential for therapeutic use of siRNA. Among the delivery systems, local delivery has advantages over systemic administration. In this study, we developed and characterized non-viral carriers to deliver siRNA locally, based on polyethylenimine (PEI) as gene carrier, and a self-assembling drug delivery system that forms a gel *in situ*. Liquid crystalline formulations composed of monoglycerides (MO), PEI, propylene glycol (PG) and 0.1 M Tris buffer pH 6.5 were developed and characterized by polarized light microscopy, Small Angle X-ray Scattering (SAXS), for their ability to form inverted type liquid crystalline phases (LC_2) in contact with excess water, water absorption capacity, ability to complex with siRNA and siRNA release. In addition, gel formation *in vivo* was determined by subcutaneous injection of the formulations in mice. In water excess, precursor fluid formulations rapidly transformed into a viscous liquid crystalline phase. The presence of PEI influences the liquid crystalline structure of the LC_2 formed and was crucial for complexing siRNA. The siRNA was released from the crystalline phase complexed with PEI. The release rate was dependent on the rate of water uptake. The formulation containing MO/PEI/PG/Tris buffer at 7.85:0.65:76.5:15 (w/w/w/w) complexed with 10 μM of siRNA, characterized as a mixture of cubic phase (diamond-type) and inverted hexagonal phase (after contact with excess water), showed sustained release for 7 days *in vitro*. In mice, *in situ* gel formation occurred after subcutaneous injection of the formulations, and the gels were degraded in 30 days. Initially a mild inflammatory process occurred in the tissue surrounding the gel; but after 14 days the tissue appeared normal. Taken together, this work demonstrates the rational development of an *in situ* gelling formulation for local release of siRNA.

1. Introduction

RNA interference (RNAi) has attracted much attention as a new approach for the treatment of many genetic and nongenetic human diseases since 1998, when Fire, Mello and colleagues (Fire et al., 1998) discovered that double-stranded RNAs could silence target gene expression in the nematode worm *Caenorhabditis elegans*. However, the clinical applicability of RNAi is limited due to various challenges related to the delivery of short interfering RNA (siRNA) molecules, which specifically induce the degradation of complementary messenger RNA in the cytosol. The development of a clinically useful, safe and effective carrier system is required (Guzman-Villanueva et al., 2012; Peer and Lieberman, 2011). The essential design criteria for non-viral siRNA carriers include neutralization of the negatively charged phosphate backbone of nucleic acids to avoid charge repulsion by the anionic cell membrane, an appropriate size for cellular internalization, protection of the nucleic acids from nuclease degradation and promotion of endosomal escape (Wong et al., 2007).

* Corresponding author.
E-mail address: vbentley@usp.br (M.V.L.B. Bentley).

http://dx.doi.org/10.1016/j.ejps.2015.04.017
0928-0987/

Compared to local delivery, systemic administration of siRNA meets several additional challenges that must be overcome by the carrier, such as interaction of the formulation with blood components, their uptake by clearance tissues, and escape from the blood stream into the target tissue (Peer and Lieberman, 2011). In this context, local delivery has several advantages, including the potential use of lower doses, a decreased risk of premature clearance, a more sustained silencing effect, site-specific delivery and decreased immunostimulation (Guzman-Villanueva et al., 2012; Vicentini et al., 2013).

Among local administration systems, self-assembling formulations, such as *in situ* gelling delivery systems, have become an attractive approach for the release of nucleic acids including DNA plasmids (Li et al., 2003) and siRNAs (Borgheti-Cardoso et al., 2014; Han et al., 2011; Kim et al., 2012; Krebs et al., 2009; Nguyen et al., 2013). These *in situ* gelling delivery systems are minimally invasive and less painful compared with solid implants because they can be injected through a syringe into the body, and they form a viscous gel *in situ* only after injection (Packhaeuser et al., 2004). The gel formation is important to limit systemic redistribution and can promote sustained release.

In situ gelling systems for siRNA delivery have previously been based on *in situ* crosslinking or precipitation through a stimulus-dependent sol–gel transition (Han et al., 2011; Krebs et al., 2009). Although these systems retained siRNA locally, release of siRNA from the gels was not easily controlled. Moreover, siRNA was released unprotected and without helper molecules, which results in a short *in vivo* half-life and low gene silencing efficiency (Kim et al., 2012; Nguyen et al., 2013). Moreover, the *in situ* crosslinking and precipitation of these systems can harm tissues and the siRNA cargo (Packhaeuser et al., 2004).

In contrast, *in situ* solidifying organogels that take advantage of *in situ* solidification under biological conditions at the site of administration can overcome these drawbacks. The organogels can be generated from amphiphilic lipids such as monoglycerides (MO) that swell in the presence of water and form various types of lyotropic liquid crystals (Agarwal and Rupenthal, 2013; Hatefi and Amsden, 2002; Yaghmur et al., 2013). Previously, our group developed MO-based delivery systems for siRNA delivery using oleylamine (OAM) as gene carrier. The MO-OAM-based delivery systems complexed the siRNA and formed a gel *in vivo* after subcutaneous injection, showing that these delivery systems can be potentially used for siRNA release (Borgheti-Cardoso et al., 2014). Further studies were performed to evaluate the release of siRNA, the system containing MO/OAM/PG/tris buffer 8.16:0.34:76.5:15 (w/w/w/w) did not release siRNA during 7 days (data not published). In this study, aiming to maintain the advantages of *in situ* solidifying organogels and to promote and optimize the siRNA delivery, the cationic polymer polyethylenimine (PEI) instead of OAM was used as gene carrier to obtain a MO-based delivery system. PEI has been widely used as gene carrier due to its ability to promote *in vitro* and *in vivo* transfection (Yin et al., 2014).

The presence of additives can influence the liquid crystalline phase formation (Borgheti-Cardoso et al., 2014; Rossetti et al., 2011) and consequently the drug release. Therefore, the effects of addition or conjugations of the PEI to the MO-based precursor fluid formulation on the packing parameters of MO and the resulting liquid crystalline phase were evaluated by polarized light microscopy and Small Angle X-ray Scattering (SAXS). The optimized precursor fluid formulations were characterized for their water absorption profiles, ability to complex siRNA and to maintain its stability, and *in vitro* siRNA release profiles. Finally, the ability to form a liquid crystalline gel, the biocompatibility and the disappearance of the formed gel after subcutaneous injection in an animal model were evaluated.

2. Materials and methods

2.1. Materials

Monoglycerides (MO, Myverol 18–92 K consisting of 93% of monoglycerides (containing 65% glyceryl monolinoleate, 23% glyceryl monooleate, 6% monoglyceride (C16), 4% monoglyceride (C18), 1% monoglyceride (C20) and 1% monoglyceride (C18:3)), 6% of diglycerides and triglycerides following the same fatty acid profile as the MO and other minor components (<1%) of free fatty acids and glycerol and trace amount of citric acid, ascorbic acid and tocopherols) was kindly provided by Kerry Bio Science (Zwijndrecht, The Netherlands). Branched polyethylenimine (25 kDa), diethyl pyrocarbonate (DEPC), ethidium bromide and isopentane were all purchased from Sigma Aldrich Co. (St. Louis, MO, USA). Propylene glycol (PG) was obtained from Labsynth Produtos by Laboratórios Ltda (Diadema, SP, Brazil). Ultrapure™ Agarose was purchase from Invitrogen™ (Carlsbad, CA, USA). *Silencer* Negative Control #1 siRNA (Catalogue #AM4635) was purchased from Ambion (Austin, TX, USA). Heparin was purchased from Blausiegel (Cotia, SP, Brazil). Kapton was obtained from E.I. DuPont de Nemours & Co., Inc. (Wilmington, Delaware, USA). Tris(hydroxymethyl)aminomethane was purchased from Merck KGaA (Darmstadt, Germany). Dialysis tubing with a 50,000 molecular weight cut-off was obtained from Spectrum Laboratories, Inc. (Rancho Dominquez, CA, USA).

2.2. Methods

2.2.1. Preparation of precursor fluid formulations

The precursor fluid formulations were prepared by mixing pre-warmed (42 °C) MO with PG in proportions of 1:9 to 9:1 (w/w). Immediately thereafter, Tris buffer pre-warmed to 42 °C, was weighted and added at concentrations ranging from 5% to 90%. For the systems containing the cationic polymer, PEI was mixed with MO in the following ratios: 12:1, 6:1 and 3:1 (MO/PEI; (w/w)). PG was then incorporated under vortex stirring, and Tris buffer was finally added as described above. The resulting formulations MO/PG/Tris buffer and MO/PEI/PG/Tris buffer (here after referred to as MO/PEI, for the sake of clarity) were stored in closed vials at room temperature.

2.2.2. In vitro inverted type liquid crystalline phase formation assay

Homogeneous and stable fluid formulations were selected for the *in vitro* gelling test that was performed by combining 100 μL of these formulations with excess water (900 μL) at 37 °C. The inverted type liquid crystalline phases (LC_2) formed in excess water were stored in closed vials for 7 days.

2.2.3. Phase behavior

2.2.3.1. Polarizing light microscopy studies. Precursor fluid formulations and LC_2 formed after contact with excess water were macroscopically characterized by visual analysis and microscopically examined under a polarized light microscope (Axioplan 2 Image Pol microscope, Carl Zeiss, Oberkichen, Germany) after 24 h and 7 days (data not shown for precursor fluid formulations) at 25 °C.

2.2.3.2. Small angle X-ray scattering (SAXS). The crystalline structure of the LC_2 formed after 24 h of contact with excess water was determined by SAXS. The analysis was performed by placing the samples in a sample holder between Kapton sheets. The scattering angle measurements were performed at a wavelength of 0.1608 nm using the D02A-SAXS beamline at the Brazilian Synchrotron Light Laboratory (LNLS), Campinas, Sao Paulo, Brazil. The scattered intensity curves were recorded using a two-

dimensional Pilatus detector with a measurement time of 300 s, q-range of 0–3 nm^{-1}, at room temperature. The intensity measurements were performed as a function of the scattering vector q [$q = (4\pi\sin\theta)/\lambda$]. The results were corrected by a detector response, and the SAXS data were normalized to take into account the transmission for each case. The scattering from the Kapton sheets in the sample holder was also removed.

2.2.4. Swelling studies

The swelling studies were performed gravimetrically. The precursor fluid formulations (100 μL) were placed in a dialysis tube (50,000 Da cut off) that was introduced into 3 mL water and maintained at 37 °C in a water bath. At fixed time intervals (15 and 30 min and 1, 2, 4, 8, 12, 24 and 48 h), each dialysis tube was removed. The surface of the dialysis membrane was blotted with a piece of fine weave paper to remove any excess water and subsequently weighed. The water uptake data were fitted according to the first (Eq. (1)) and second (Eq. (2)) order kinetics equations for swelling studies (Lara et al., 2005; Rizwan et al., 2009).

$$\ln\frac{W_\infty}{W_\infty - W} = kt \quad (1)$$

$$\frac{t}{W} = \frac{1}{kW_\infty^2} + \frac{t}{W_\infty} \quad (2)$$

W is the water uptake at time t, W_∞ is the maximum water uptake, k is the rate constant, and (W_∞–W) is the unrealized water uptake. For the second-order equation, the maximum or equilibrium water uptake (W_∞) of the MO can be described using the reciprocal of the slope, and the initial rate of swelling is the reciprocal of the y-intercept of the plot t/W versus t (Lara et al., 2005; Rizwan et al., 2009).

2.2.5. siRNA loading and its stability in the precursor fluid formulation

To determine if the precursor fluid formulations were capable of complexing siRNA, *Silencer* Negative Control #1 siRNA (siRNA) was used and added to the precursor fluid formulations at a final concentration of 10 μM. The mixtures were incubated at room temperature for 30 min. A 40 μL aliquot of this mixture or the control (siRNA in DEPC-treated water) was added to 10 μL of loading buffer (Bromophenol blue (0.25%, p/v), xylene cyanol FF (0.25%,p/v), Orange G (0.25%, p/v), Tris–HCl pH 7.5 (10 mmol/L), ethylenediamine tetraacetic acid (10 mmol/L) and saccharose (0.65%, p/v)). Then, 40 μL of each mixture was subjected to electrophoresis in an ethidium bromide-stained Tris-acetate–EDTA(TAE)-buffered 2% agarose gel at 100 V for 20 min followed by visualization under UV light (Tran et al., 2008).

The stability of the siRNA in the precursor fluid formulations was analyzed using a heparin polyanion competition assay (Shen et al., 2011). For this, siRNAs complexed with the formulations were prepared as described above. To determine the appropriate volume of heparin to promote decomplexation of the siRNA, different volumes (3.2, 10 and 20 μL) of heparin (5000 U.I./mL) were added to 40 μL of the formulations. It was determined that a volume of 10 μL of heparin was sufficient to compete with the siRNA and to promote its decomplexation in most systems, with the exception of the MO/PEI 15.69:1.31 (w/w) system, which required 20 μL (data not shown). Therefore, for the heparin polyanion competition assay, either 10 μL or 20 μL of heparin was added to the formulations with agitation. These mixtures were incubated at 37 °C for 1 h. The solutions were then subjected to electrophoresis on agarose gels as described above.

2.2.6. In vitro siRNA release from the LC_2s

Release studies were performed in 12-well plates with an insert with 1.0 μm pore size. A 100 μL aliquot of the precursor fluid formulations (or DEPC-treated water as a control) containing 10 μM siRNA was added to the insert. The receiving medium in the well consisted of 1800 μL of DEPC-treated water maintained at 37 °C. Receiving media was removed at specific time intervals (24, 48 h and 7 days) and replaced with fresh DEPC-treated-water. At the end of the experiment, samples were dried in an Eppendorf 5301 Concentrator, and resuspended in DEPC-treated water (60 μL) and divided into two Eppendorf tubes. In one tube, 10 μL of heparin (5000 U.I./mL) was added for the polyanion competition assay. In the second tube, 10 μL of DEPC water was added, and the samples were incubated at 37 °C for 1 h. The released siRNA was analyzed qualitatively by agarose gel electrophoresis as described in the previous section. For the quantification of the released siRNA, a standard curve (15–0.9375 μM siRNA) was also electrophoresed. The signal intensities of the standards and samples in each agarose gel were calculated using NIH ImageJ software (http://rsbweb.nih.gov/ij/).

2.2.7. In situ gel formation and biocompatibility study in mice

Female BALB/c mice (18–20 g) were used to study the *in situ* gelling ability of the precursor fluid formulations after subcutaneous injection. All animals were maintained under standard environmental conditions (20–24 °C and 12 h:12 h light–dark cycle) with access to food and water *ad libitum*. The experimental protocol was approved by the Ethics Commission for the Use of Animals (CEUA) of the Campus of Ribeirao Preto, University of Sao Paulo, Ribeirao Preto, SP, Brazil (Protocol No. 10.1.1749.53.8). A 50 μL aliquot of the precursor liquid formulation sterilized by membrane filtration (pore size 0.2 μm) was injected subcutaneously into the dorsal flank of BALB/c mice. The mice were sacrificed after injection at predetermined time intervals (24, 48 and 72 h and 7, 14 and 30 days), and gel formation in the subcutaneous region was evaluated as a function of the formation time and persistence in the tissue. The presence of the gel at the injection site was recorded using a Sony camera model DSC-WX9. The gels were also evaluated under a polarized light microscope 24 h after the subcutaneous injection to characterize the crystalline liquid structure formed.

For the biocompatibility studies, samples of the skin, were studied at the end of the experiment. The samples were placed under a support tissue, and immediately frozen in isopentane cooled in liquid nitrogen and stored at −80 °C. Histological sections (5 μm) were cut in a cryostat (Leica CM1850, Leica Microsystems Nussloch GmbH, Nussloch, Germany) and mounted on extra-white gelatinized glass slides. The slides were stained with hematoxylin–eosin (H&E) for histological analysis using a motorized Olympus BX61 microscope (Olympus America Inc., Melville, New York, USA) attached to an Olympus DP 72 camera.

2.2.8. Statistical analysis

Significant differences between two groups were analyzed using t-tests. Comparisons between more than two groups were made using one-way ANOVA with a Tukey post hoc test. Statistical differences were considered significant when $p < 0.05$.

3. Results and discussion

3.1. Characterization of the precursor fluid formulations by polarized light microscopy

The liquid crystalline structure of the systems composed of MO, PEI, PG and Tris buffer were characterized macroscopically and by polarized light microscopy 24 h after preparation. A ternary diagram or Gibbs Triangle, which works as a map for navigating between the different phases (Kulkarni et al., 2011) was constructed from the macro- and microscopic analyses of the systems

composed of MO/PG/Tris buffer (Fig. 1A) and MO/PEI/PG/Tris buffer with MO/PEI ratios of 12:1 (Fig. 1B), 6:1 (Fig. 1C) and 3:1 (Fig. 1D) (w/w). Over the years, binary and ternary phase diagrams of MO were constructed for purposes of phase identification and structure characterization (Chang and Bodmeier, 1998; Clogston et al., 2000; Landh, 1994; Qiu and Caffrey, 2000). This information help understanding and exploring the liquid crystalline systems (LCSs) obtained from MO as a drug delivery system.

As shown in Fig. 1, different proportions and type of components resulted in distinct systems, characterized as cubic (gel optically isotropic), hexagonal (fanlike structure and birefringence) and lamellar phases (as oily streaks with inserted maltese crosses), isotropic liquid, emulsion (droplet), unstable emulsion and transition phase (a mixture of isotropic, birefringence and droplets) after macroscopic and polarized light microscopic analysis. These results show that it is possible to obtain MO/PEI-based fluid systems that

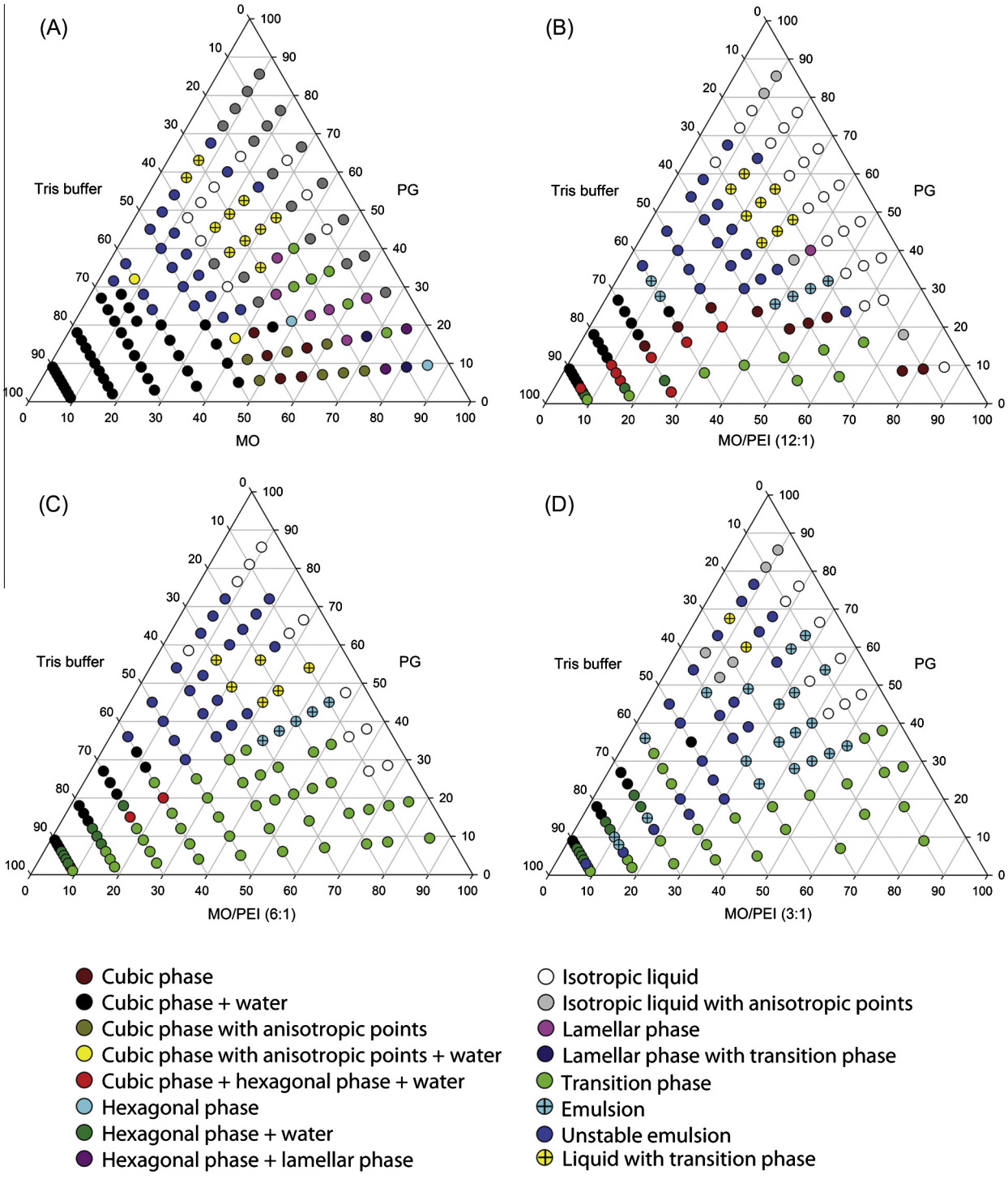

Fig. 1. Ternary phase diagram of (A) MO/PG/Tris buffer, (B) MO/PEI(12:1)/PG/Tris buffer, (C) MO/PEI(6:1)/PG/Tris buffer and (D) MO/PEI(3:1)/PG/Tris buffer at 24 h. MO (monoglycerides), PEI (polyethylenimine), PG (propylene glycol). Samples were prepared and store at room temperature. Polarized light microscopy analysis were performed at 25 °C.

can transform into viscous LCSs in contact with excess water. The region of homogenous fluid formulation characterized as isotropic in polarized light microscopy was defined as an isotropic liquid phase. This phase was observed at lower Tris buffer concentration (white circles in Fig. 1) while at higher Tris buffer concentrations a gel in equilibrium with excess water was formed. This gel (Diagram A) showed an isotropic structure in polarized light microscopy and was characterized as a bicontinuous cubic phase. The bicontinuous cubic phase was also observed with the addition of low concentrations of PEI (black circle in Fig 1B–D). At higher proportions of MO/PEI, the formation of an inverted hexagonal phase or loss of liquid crystalline structure was observed.

The presence of isotropic liquid and bicontinuous cubic phase at lower and higher solvent content, respectively, was also reported by Chang and Bodmeier (1998), who concluded that the isotropic liquid phase can be transformed into the bicontinuous cubic phase after injection due to their ability to absorb fluids from the body (Chang and Bodmeier, 1998). The ability of low-viscous systems to transform to inverted-type highly organized hierarchical structures (such as inverted hexagonal phase and bicontinuous cubic phase) upon exposure to biological environment render them useful for controlled release of drugs *in situ* (Yaghmur et al., 2013). The dynamic structural transition from low-viscous system to high-viscous system was evaluated by Yaghmur et al. (2011). The results showed that the time required for the water diffuse to the sample is fast (2–3 min), inducing a fast rearrangement of the lipid and the drug molecules in excess phosphate buffer followed by a total conversion of the low-viscous system to the fully hydrated inverted hexagonal phase. After 1000 s, the equilibrated fully hydrated system was reached (Yaghmur et al., 2011). It is important to notice that other studies required a longer time (24 h and 7 days) to reach the equilibration condition (Han et al., 2010; Lara et al., 2005; Rizwan et al., 2009).

This change from a less viscous phase into a bicontinuous cubic structure or inverted hexagonal phase can be explained by the critical packing parameter (cpp). The cpp relates the shape of the molecule to properties that influence the curvature of the polar-nonpolar interface and consequently the type of aggregate formed. Therefore, the cpp is a useful parameter for predicting the mesophase that is preferably formed by an amphiphile and can be calculated via Eq. (3).

$$\mathrm{cpp} = v_s / a_o l_c \tag{3}$$

where cpp represents the critical packing parameter, v_s is the hydrophobic chain volume, a_o is the polar head group area, and l_c is the chain length (Mitchell and Ninham, 1981). When the l_c is constant, the mesophases are influenced primarily by v_s and a_o, and the addition of other compounds can influence these parameters, which may result in a change in the structure of the phase formed (Chang and Bodmeier, 1997a). The cpp values are usually ~1 for the lamellar phase (Engstrom and Engstrom, 1992), ~1.3 for the bicontinuous cubic phase and ~1.7 for the inverted hexagonal phase (Larsson, 1989).

The increase in water content allows the polar head groups of MO to move more freely in a perpendicular direction relative to the plane of the water layer. These movements promote disorder in the hydrophobic chain of MO, thereby increasing v_s. Because the interaction of the polar head groups is strong, due to hydrogen bonding, their cross section tends to be constant. Therefore, the packing factor increases because v_s increases, whereas a_o and l_c are constant, thereby facilitating the transformation from a lamellar to a cubic phase (Amar-Yuli and Garti, 2005).

The addition of drugs or solvents was reported to change the liquid crystalline phases. The characteristics of the added compound will determine whether it will be located at the polar or nonpolar domains of the systems (Chang and Bodmeier, 1998; Engstrom and Engstrom, 1992; Landh, 1994; Liu et al., 2013; Mezzenga et al., 2005; Rossetti et al., 2011). The change in liquid crystalline phases due to the presence of the additive at the polar or nonpolar domain of the system may be explained by the cpp. Generally, addition of hydrophilic and charged compounds favors lamellar phases due to an increase in a_o (Engstrom and Engstrom, 1992; Liu et al., 2013), while the addition of nonpolar drugs, which strongly partition into the nonpolar domain, increasing v_s, tend to favor the formation of cubic and hexagonal phases (Fong et al., 2012; Phan et al., 2011). However, a hexagonal phase can also be formed after addition of hydrophilic or charged drugs (Mezzenga et al., 2005; Yaghmur et al., 2007). Mezzenga et al. (2005) demonstrated that glucose, a hydrophilic compound, may change the a_o through strong hydrogen bonding. They showed that, the monolayer of the lipid–water interface of the lamellar phase was changed to a cubic phase by the presence of glucose, or similarly, the curvature of the cubic phase was reduced and transformed to the inverted hexagonal phase (Mezzenga et al., 2005). The presence of higher concentrations of charged peptide surfactants also favored the change from cubic to inverted hexagonal phase (Yaghmur et al., 2007). Hence, due to the complexity of the lipid–water system, it is difficult to predict which liquid crystalline phase is formed. Several issues have to be evaluated such as concentration, size, degree of hydrophobicity and ionic strength of the components of the system and the location of the components at the polar or nonpolar domain of the system.

3.2. In vitro inverted type liquid crystalline phase formation assay

All precursor fluid formulations characterized as isotropic liquids (white circles in Fig. 1) were analyzed, and the LC_2 obtained in the *in vitro* gelling test were characterized macroscopically and using polarized light microscopy. All of the LC_2 obtained from the formulations of MO/PG/Tris buffer showed isotropic characteristics for 7 days. However, when PEI was added, the LC_2 formed from the precursor fluid formulations (white circles in Fig. 1B–D) changed. At lower concentrations of PEI, the LC_2 were characterized as a bicontinuous cubic phase, at intermediate concentrations, the LC_2 existed as an inverted hexagonal phase, and at higher concentrations, the formation of liquid crystalline phases did not occur. The excess concentrations of PEI harmed the formation of LCSs probably because the increasing charge at the polar domains disturbs the organization of the liquid crystalline structures. It was reported that the addition of a high concentration of glycerol to the continuous water phase decreased the degree of order inside the particles, which affected the hexagonal phase formed from phytantriol (Engelskirchen et al., 2011).

After selecting the precursor fluid formulations that formed LC_2 when they were in contact with excess water, a detailed *in vitro* gelling test was performed to characterize the LC_2 at 24, 48, 72 h and 7, 10 and 14 days after formation macroscopically and by polarizing light microscopy. The LC_2 obtained from the formulations containing 5.57%, 6.46%, 7.85% and 15.69% MO remained stable for up 24 h after contact with excess water (Table 1). Moreover, the systems containing 7.85% and 15.69% MO had visibly greater gel volumes.

Considering the possible cytotoxicity of PEI (Liu et al., 2011), lower concentrations of PEI were also tested in the chosen formulations (Table 1). The precursor fluid formulations obtained were characterized as fluid and homogenous systems at 24 h, and again, higher PEI concentrations influenced the liquid crystalline phase formed (Table 1). Notably, at lower PEI concentrations the structure of the formed LC_2 was not affected and remained in the bicontinuous cubic phase. The influence of PEI on liquid crystalline phase will be better discussed in Section 3.3.

Table 1
Characteristics of LC_2 formed from precursor formulations with excess water as determined by polarized light microscopy at 24, 48 and 72 h and 7, 10 and 14 days at 25 °C.

MO%	PEI/PG/Tris buffer%	Structural identification of the gel formed/time in contact with excess water
5.57	0.93:58.50:35.00	CP with anisotropic points/24–72 h HP/7–14 days
5.57	0.46:58.50:35.47	CP with anisotropic points/24–72 h HP/7–14 days
5.57	0.23:58.50:35.70	CP with anisotropic points/24–72 h HP/7–14 days
5.57	0.09:58.50:35.84	CP/24 h–14 days
6.46	0.54:63.00:30.00	CP with anisotropic points/24–72 h HP/7–14 days
6.46	0.27:63.00:30.27	CP with anisotropic points/24–72 h HP/7–14 days
6.46	0.13:63.00:30.41	CP with anisotropic points/24–72 h HP/7–14 days
6.46	0.05:63.00:30.49	CP/24 h–14 days
7.85	0.65:76.50:15.00	HP/24 h–7 days Milky solution[a]/10–14 days
7.85	0.32:76.50:15.33	HP/24 h–7 days Milky solution[a]/10–14 days
7.85	0.16:76.50:15.49	CP/24–72 h HP/7–14 days
7.85	0.06:76.50:15.59	CP/24 h–14 days
15.69	1.31:68.00:15.00	HP/24–72 h Milky solution[a]/7–14 days
15.69	0.65:68.00:15.66	HP/24 h–14 days
15.69	0.33:68.00:15.98	HP/24 h–14 days
15.69	0.13:68.00:16.18	CP/24 h–14 days

CP: cubic phase, HP: hexagonal phase, MO: monoglycerides, PEI: polyethylenimine, PG: propylene glycol.
[a] In these systems, changes from viscous liquid crystalline phases (HP) to milky solutions were observed.

Based on these results, the formulations containing 7.85% and 15.69% MO were chosen for subsequent studies. With these MO and PEI compositions, it was possible to evaluate the influence of the amounts of both the main lipid component responsible for LC_2 formation (MO) and the siRNA complexing agent (PEI). In addition, these formulations, which have the highest gel volume, are expected to have a longer persistence in the tissue and exhibit prolonged siRNA release.

3.3. Small angle X-ray scattering (SAXS)

The ability to load and release drugs and to interact with biomembranes is closely associated with the inner structure and the additives present in the LCSs (Rossetti et al., 2011; Yaghmur et al., 2013). In the present study, the LC_2 formed from the precursor fluid formulations were analyzed by SAXS to determine the internal structure of the LCSs through calculation of the interplanar distances value d using Bragg's law. These distances were then correlated with the Miller indices of structure symmetry. We evaluated the effects promoted by the addition of PEI and 10 μM siRNA to the liquid crystalline structure.

The diffraction peaks obtained for the LC_2 formed from the precursor fluid formulations with or without PEI and siRNA (plots of the intensity versus the scattering vector q) (Fig. 2) allowed us to identify the liquid crystalline phase of the samples (Table 2) and to determine the lattice parameters (Table 3).

The structures of the LC_2 formed without PEI or siRNA were characterized by polarized light microscopy as bicontinuous cubic phase, which is consistent with the SAXS results. The scattering patterns of the LC_2 formed from MO/PG/Tris buffer (7.85:76.5:15.65 and 15.69:68:16.31 w/w/w) showed that two bicontinuous cubic phase is formed. The first one exhibited Bragg peaks with the relative ratios of $\sqrt{2}$:$\sqrt{3}$:$\sqrt{4}$:$\sqrt{5}$:$\sqrt{6}$:~$\sqrt{8}$:$\sqrt{9}$: and $\sqrt{3}$:$\sqrt{4}$:$\sqrt{7}$:, indicative of a diamond-type cubic phase (Pn3m space group) and a gyroid-type cubic phase (Ia3d space group), respectively. The second bicontinuous cubic phase exhibited Bragg peaks with the relative ratios of $\sqrt{2}$:$\sqrt{3}$:$\sqrt{4}$: (Lindblom and Rilfors, 1989). Previous reports showed that a gyroid-type cubic phase is obtained when the system is not in excess water (usually 10–30% of water at 20–40 °C), while the diamond-type cubic phase exists in excess water (usually 40–50% of water at 20–40 °C) (Clogston et al., 2000; De Campo et al., 2004; Qiu and Caffrey, 2000; Zabara et al., 2011; Zheng et al., 2003). It was described that increasing water content induces a transition from the Ia3d phase to the Pn3m cubic phase in systems formed by glyceryl monolinoleate-water (Mezzenga et al., 2005; De Campo et al., 2004), glyceryl monooleate–water (Qiu and Caffrey, 2000) and Myverol 18-99-water (Clogston et al., 2000). Therefore, it was expected that these LC_2 formed from the precursor fluid formulations in excess water exhibited only diamond-type cubic phases because the MO used was Myverol® 18–92 K, which consists primarily of 65% glyceryl monolinoleate and 23% glyceryl monooleate. However, a mixture of diamond and gyroid-type cubic phases was observed. It is worth to note that the presence of Ia3d and Pn3m cubic structures in equilibrium with excess water could also be observed in ternary systems formed by glyceryl monooleate/n-octyl-β-$_D$-glucopyranoside/water (Persson et al., 2003). Generally, cubic phase properties can be tuned by altering the water content, temperature and pressure or by adding charged lipids or surfactant. It is important to mention that small changes in composition or temperature are already sufficient to promote transitions between bicontinuous liquid crystalline phases (Milak and Zimmer, 2015).

In the present study, the origin of the gyroid-type cubic phase is subject to speculation. As a mixture of gyroid- and diamond-cubic phases was formed in all LC_2, except for the MO/PEI 7.85:0.65 (w/w) with siRNA and MO/PEI 15.69:1.31 (w/w) with and without siRNA, the presence of PEI and siRNA can be excluded as possible components favoring the formation of Ia3d structure in excess of water. More likely, other components of the Myverol® 18–92 K or the PG in the formulation may result in a gyroid-cubic phase in excess water. It is important to point out that the other components of Myverol® 18–92 K (12%) are mainly monoglycerides and diglycerides with hydrocarbon tails and head groups similar to the glyceryl monolinoleate and glyceryl monooleate. Hence, it is expected that the presence of these components should not affect the structure of cubic phase. On the other hand, due to its small size and two hydroxyl groups, PG could fit into the water channels, thereby favoring the formation of gyroid- and diamond-cubic phases in excess water. However, further SAXS experiments are required to elucidate whether PG is actually responsible for this phenomenon.

Different components in the formulation can affect the type of the liquid crystalline structure (Caboi et al., 2001; Chang and Bodmeier, 1997a). The addition of components to the liquid crystalline phases can manifest as either complete phase changes or as alterations in the lattice parameter. The polarity and the molecular structure of the added compound determine whether it is located at the polar interface or the nonpolar region of the lipid layer, which affects the packing ratio. The increase in the lattice parameter can be due to the hydration of the structures. Enlargement of the lattice parameter can result from the presence of hydrophilic molecules in the aqueous domains, but also from the presence of amphiphilic molecules between the polar and nonpolar groups of the reversed micelles. On the other hand, a reduction in the lattice parameter value suggests the dehydration of the aqueous domains, and their maintenance indicates the presence of hydrophobic molecules located in the hydrocarbon chains of MO or the adsorption of molecules on the surface of the reversed

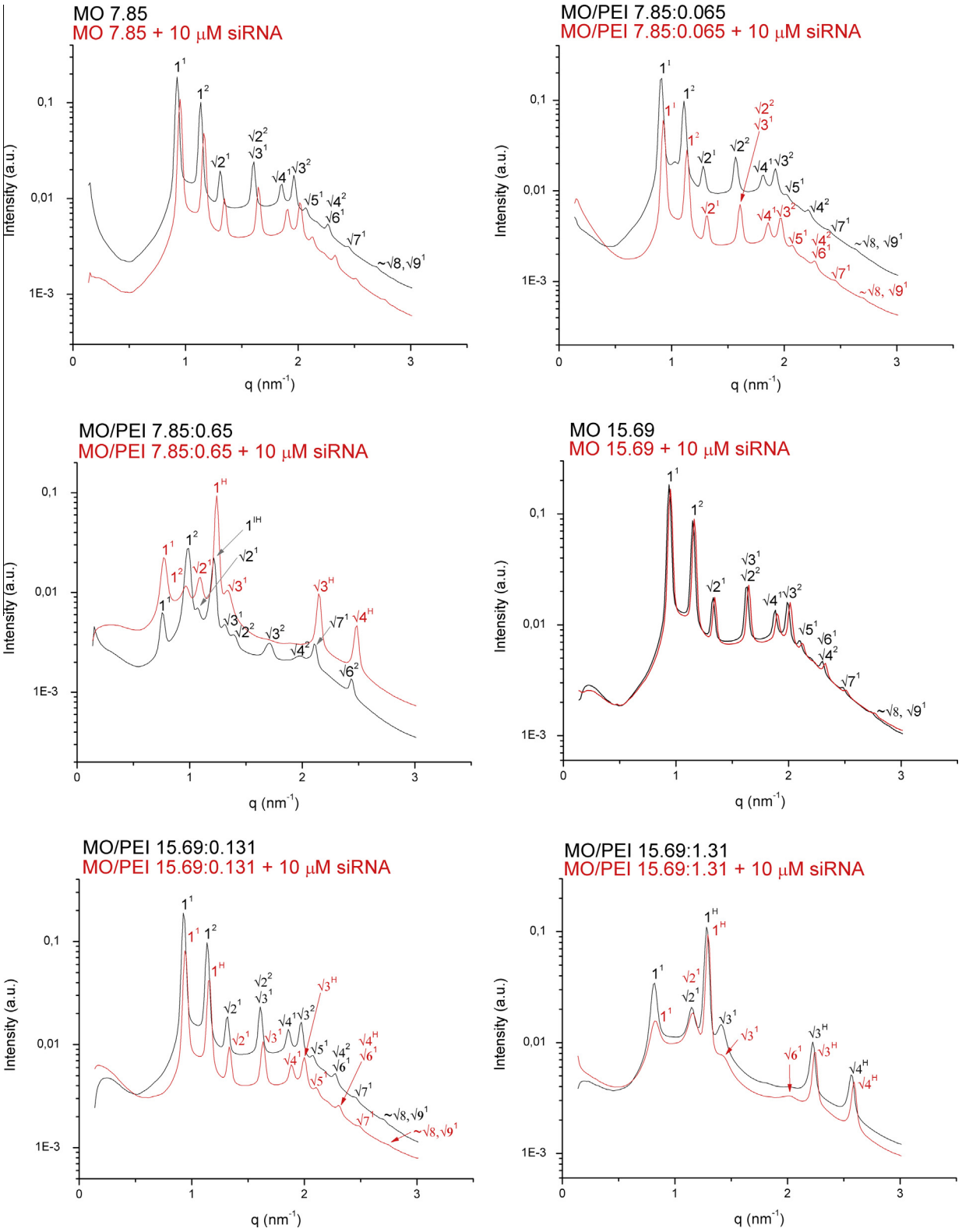

Fig. 2. SAXS results for the inverted type liquid crystalline system obtained from precursor fluid formulations composed of MO/PEI/PG/Tris buffer (w/w/w/w) and control (MO/PG/Tris buffer (w/w/w)) with and without addition of 10 μM siRNA. SAXS evaluation was performed at room temperature. For the graphic of precursor fluid formulations that presented the same relative ratios of Bragg peaks with and without siRNA, only one relative rate is indicated for better clarity. [1]: cubic phase 1; [2]: cubic phase 2; [H]: inverted hexagonal phase; [IH]: interstice of inverted hexagonal phase.

micelles (Amar-Yuli et al., 2008, 2007; Libster et al., 2007; Rossetti et al., 2011). Although, several reports claim an increase in the lattice parameter due to the presence of hydrophilic molecules in the aqueous domain, the presence of hydrophilic molecules can also promote the opposite effect, i.e., reduction in the lattice parameter. This happens when the ability of the hydrophilic molecule to bind the water is higher than the MO; this competition leads to MO dehydration, thereby reducing the effective size of the MO head

Table 2
SAXS data for different systems of MO/PG/Tris buffer and MO/PEI/PG/Tris buffer without and with siRNA (10 μM).

Sample	Without siRNA				10 μM siRNA			
	d (nm)	Ratio	CP	Structure	d (nm)	Ratio	CP	Structure
MO/PG/Tris buffer 7.85:76.5:15.65	6.7940	1:1	C1	Cubic D + G	6.6066	1:1	C1	Cubic D + G
	5.5377	1:1	C2	Cubic D	5.4126	1:1	C2	Cubic D
	4.8144	1:√2	C1	Cubic D	4.6735	1:√2	C1	Cubic D
	3.9107	1:√2	C2	Cubic D	3.8172	1:√2	C2	Cubic D
		1:√3	C1	Cubic D + G		1:√3	C1	Cubic D + G
	3.3857	1:√4	C1	Cubic D + G	3.2926	1:√4	C1	Cubic D + G
	3.2045	1:√3	C2	Cubic D	3.1211	1:√3	C2	Cubic D
	3.0418	1:√5	C1	Cubic D	2.9665	1:√5	C1	Cubic D
	2.7773	1:√4	C2	Cubic D	2.6991	1:√4	C2	Cubic D
		1:√6	C1	Cubic D		1:√6	C1	Cubic D
	2.5689	1:√7	C1	Cubic G	2.5018	1:√7	C1	Cubic G
	2.3314	∼1:√8, √9	C1	Cubic D	2.2653	∼1:√8, √9	C1	Cubic D
MO/PEI/PG/Tris buffer 7.85:0.065:76.5:15.585					6.7940	1:1	C1	Cubic D + G
	6.8917	1:1	C1	Cubic D + G	5.5377	1:1	C2	Cubic D
	5.6687	1:1	C2	Cubic D	4.8144	1:√2	C1	Cubic D
	4.9131	1:√2	C1	Cubic D	3.9107	1:√2	C2	Cubic D
	4.0088	1:√2	C2	Cubic D		1:√3	C1	Cubic D + G
	3.4590	1:√4	C1	Cubic D + G	3.3857	1:√4	C1	Cubic D + G
	3.2702	1:√3	C2	Cubic D	3.1833	1:√3	C2	Cubic D
	3.1009	1:√5	C1	Cubic D	3.0418	1:√5	C1	Cubic D
	2.8433	1:√4	C2	Cubic D	2.7773	1:√4	C2	Cubic D
	2.6252	1:√7	C1	Cubic G		1:√6	C1	Cubic D
	2.3895	∼1:√8, √9	C1	Cubic D	2.5689	1:√7	C1	Cubic G
					2.3314	∼1:√8, √9	C1	Cubic D
MO/PEI/PG/Tris buffer 7.85:0.65:76.5:15	8.3293	1:1	C1	Cubic D + G				
	6.3442	1:1	C2	Cubic D	8.1870	1:1	C1	Cubic D
	5.8774	1:√2	C1	Cubic D	6.5168	1:1	C2	Cubic D
	5.1786	1:1		IH	5.7366	1:√2	C1	Cubic D
	4.8144	1:√3	C1	Cubic D + G	5.0690	1:1		Hexagonal
	4.4980	1:√2	C2	Cubic D	4.7196	1:√3	C1	Cubic D
	3.6710	1:√3	C2	Cubic D	2.9302	1:√3		Hexagonal
	3.1833	1:√4	C2	Cubic D	2.5282	1:√4		Hexagonal
	3.1252	1:√7	C1	Cubic G				
	2.5827	1:√6	C2	Cubic D				
MO/PG/Tris Buffer 15.69:68:16.31	6.6990	1:1	C1	Cubic D + G	6.6066	1:1	C1	Cubic D + G
	5.4744	1:1	C2	Cubic D	5.4126	1:1	C2	Cubic D
	4.7196	1:√2	C1	Cubic D	4.6735	1:√2	C1	Cubic D
	3.8479	1:√2	C2	Cubic D	3.8172	1:√2	C2	Cubic D
		1:√3	C1	Cubic D + G		1:√3	C1	Cubic D + G
	3.3385	1:√4	C1	Cubic D + G	3.3154	1:√4	C1	Cubic D + G
	3.1622	1:√3	C2	Cubic D	3.1211	1:√3	C2	Cubic D
	3.0037	1:√5	C1	Cubic D	2.9665	1:√5	C1	Cubic D
	2.7299	1:√4	C2	Cubic D	2.6991	1:√4	C2	Cubic D
		1:√6	C1	Cubic D		1:√6	C1	Cubic D
	2.5282	1:√7	C1	Cubic G	2.5018	1:√7	C1	Cubic G
	2.2979	∼1:√8, √9	C1	Cubic D	2.2760	∼1:√8, √9	C1	Cubic D
MO/PEI/PG/Tris Buffer 15.69:0.131:68:16.179	6.7940	1:1	C1	Cubic D + G	6.6990	1:1	C1	Cubic D + G
	5.5377	1:1	C2	Cubic D	5.4744	1:1		Hexagonal
	4.7665	1:√2	C1	Cubic D	4.7196	1:√2	C1	Cubic D
	3.9107	1:√2	C2	Cubic D	3.8479	1:√3	C1	Cubic D + G
		1:√3	C1	Cubic D + G	3.3385	1:√4	C1	Cubic D + G
	3.3857	1:√4	C1	Cubic D + G	3.1415	1:√3		Hexagonal
	3.1833	1:√3	C2	Cubic D	2.9850	1:√5	C1	Cubic D
	3.0226	1:√5	C1	Cubic D	2.7299	1:√4		Hexagonal
	2.7613	1:√4	C2	Cubic D		1:√6	C1	Cubic D
		1:√6	C1	Cubic D	2.5282	1:√7	C1	Cubic G
	2.5552	1:√7	C1	Cubic G	2.2869	∼1:√8, √9	C1	Cubic D
	2.3201	∼1:√8, √9	C1	Cubic D				
MO/PEI/PG/Tris buffer 15.69:1.31:68:15	7.6633	1:1	C1	Cubic D	7.6633	1:1	C1	Cubic D
	5.4744	1:√2	C1	Cubic D	5.4126	1:√2	C1	Cubic D
	4.9131	1:1		Hexagonal	4.8633	1:1		Hexagonal
	4.4562	1:√3	C1	Cubic D	4.4152	1:√3	C1	Cubic D
	2.8265	1:√3		Hexagonal	3.1211	1:√6	C1	Cubic D
	2.4506	1:√4		Hexagonal	2.7935	1:√3		Hexagonal
					2.4258	1:√4		Hexagonal

CP: cubic phase; C1: cubic phase 1; C2: cubic phase 2; IH: interstice of inverted hexagonal phase; Cubic D (bicontinuous): Pn3m and Pm3n; Cubic G (bicontinuous): Ia3d, Hexagonal: inverted hexagonal phase, MO: monoglycerides, PEI: polyethylenimine, PG: propylene glycol. Data were determined at room temperature.

Table 3
Lattice parameter average of different systems determined by SAXS.

Sample	Without siRNA Lattice parameter average (nm)	10 μM siRNA Lattice parameter average (nm)
MO/PG/Tris buffer	a_{c1} = 6.793 ± 0.013	a_{c1} = 6.610 ± 0.014
7.85:76.5:15.65	a_{c2} = 5.543 ± 0.011	a_{c2} = 5.404 ± 0.007
MO/PEI/PG/Tris buffer	a_{c1} = 6.933 ± 0.026	a_{c1} = 6.793 ± 0.014
7.85:0.065:76.5:15.585	a_{c2} = 5.672 ± 0.010	a_{c2} = 5.534 ± 0.017
MO/PEI/PG/Tris buffer	a_{c1} = 8.312 ± 0.031	a_{c1} = 8.158 ± 0.040
7.85:0.65:76.5:15	a_{c2} = 6.351 ± 0.016	a_{c2} = 6.517
	a_H = 5.980	a_H = 5.851 ± 0.012
MO/PG/Tris buffer	a_{c1} = 6.688 ± 0.016	a_{c1} = 6.619 ± 0.011
15.69:68:16.31	a_{c2} = 5.463 ± 0.016	a_{c2} = 5.404 ± 0.007
MO/PEI/PG/Tris buffer	a_{c1} = 6.765 ± 0.015	a_{c1} = 6.679 ± 0.012
15.69:0.131:68:16.179	a_{c2} = 5.526 ± 0.010	a_H = 6.321 ± 0.020
MO/PEI/PG/Tris buffer	a_c = 7.708 ± 0.040	a_c = 7.653 ± 0.008
15.69:1.31:68:15	a_H = 5.673 ± 0.012	a_H = 5.602 ± 0.014

a_{c1} = lattice parameter average of bicontinuous cubic phase 1, a_{c2} = lattice parameter average of bicontinuous cubic phase 2 and a_H = lattice parameter average of inverted hexagonal phase, MO: monoglycerides, PEI: polyethylenimine, PG: propylene glycol. Data were determined at room temperature.

groups, which is reflected in the decrease in the lattice parameter value (Amar-Yuli et al., 2007; Borgheti-Cardoso et al., 2014; Souza et al., 2014).

In this study, PEI added at low concentrations (MO/PEI at 7.85:0.065 and 15.69:0.131 (w/w)) did not alter the liquid crystalline structure when compared with formulations lacking PEI. However, it promoted an increase in the lattice parameters (Table 3), which suggests that it is located in the aqueous domain. The increase in the lattice parameter after addition of charged molecules can be attributed to the electrostatic repulsion between the charges of the molecules that are incorporated into the MO-based membrane interface. This repulsion increases the distances between the charged molecules and consequently increase the a_o value (Yaghmur et al., 2007). Higher concentrations of PEI resulted in a phase change: a bicontinuous cubic phase with an interstice of inverted hexagonal phase for the formulation composed of MO/PEI at 7.85:0.65 (w/w) and a mixture of bicontinuous cubic phase with inverted hexagonal phase for the formulation composed of MO/PEI at 15.69:1.31 (w/w). It was expected that a higher concentration of PEI would increase a_o (which was observed in Table 3) and consequently decrease cpp, favoring the formation of lamellar phase; however a mixture of bicontinuous cubic with inverted hexagonal phase was formed. This effect could be caused by the increase of the negative curvature caused by the increase of ionic strength. Liu et al. (2013) demonstrated that the increase of ionic strength from addition of saline solution screens the electrostatic repulsion between ionic molecules leading to an increase of the negative curvature that results in a transition from lamellar phase to bicontinuous cubic phase (Liu et al., 2013). It was also reported that the content of charge has to be high enough to surpass the critical value of the curvature to result in a change from bicontinuous cubic to inverted hexagonal phase (Aota-nakano et al., 1999). Hence, we conclude that the charge of PEI in these systems is high enough to cause a mixture of bicontinuous cubic and inverted hexagonal phases, but insufficient for a complete phase change. The accuracy of the SAXS analysis revealed all of the LCSs present, even those not observed under polarized light microscopy, such as the isotropic form of the bicontinuous cubic phase, which can be disguised by the birefringence of the inverted hexagonal phase.

The impact of the interaction of the siRNAs with the LCSs was also observed during the SAXS evaluation. The hydrophilicity of the siRNA could explain the decrease in the lattice parameters (Borgheti-Cardoso et al., 2014). As discussed above, the ability of the siRNA to bind water is most likely higher than the MO; therefore, MO dehydration occurs, leading to the decrease in the lattice parameter value. This effect was also observed in other studies of the addition of a highly hydrophilic polymer (hydrophilic–lipophilic balance = 17) and Poly(hexamethylene biguanide) hydrochloride to MO-based systems (Amar-Yuli et al., 2007; Souza et al., 2014). The same effect was observed in LCS obtained from phytantriol when glycerol was added (Engelskirchen et al., 2011).

3.4. Swelling studies

The swelling rate and the type of LCSs formed by swelling of the amphiphiles, such as MO, can affect the drug release kinetics. Fig. 3A shows the weight of the selected formulations expressed as a function of time. The swelling kinetics parameters (W_o: initial rate of absorption; W_∞: maximum water uptake) are summarized in Fig. 3A. The systems without PEI were used as controls.

Notably, for all tested formulations, the water uptake initially increased rapidly; after a few hours, this absorption stabilized and reached a state of equilibrium. The rapid swelling indicated that the formation of a viscous bicontinuous cubic or inverted hexagonal phase is a fast process, which is consistent with other studies (Lara et al., 2005; Rizwan et al., 2009).

As shown in Fig. 3A, the formulations with higher PEI concentrations had a greater water uptake, which is also reflected in the maximum water uptake (W_∞), as determined by the swelling kinetics. The statistical analyses of the water uptake results showed that the formulation composed of MO/PEI at 7.85:0.65 (w/w) absorbed more water than the formulation of MO/PEI at 7.85:0.065 (w/w) ($p < 0.05$ after 1 h) and the formulation without PEI ($p < 0.05$ after 30 min). The systems composed of MO/PEI at 15.69:1.31 (w/w) had a water uptake rate higher than the formulations with lower and without PEI after 4 and 2 h ($p < 0.05$), respectively. Additionally, lower concentrations of PEI (0.065% and 0.131%) in both systems exhibited the same absorption of water as the system without PEI during the entire period evaluated. Moreover, after 8 h, the same water absorption were also observed in both systems without PEI. Several authors showed that the water uptake of LCSs formed by MO is inversely proportional to the initial water content (Geraghty et al., 1996; Lara et al., 2005; Rizwan et al., 2009). Considering that the systems MO/PEI at 7.85:0.065 and 15.69:0.131 (w/w) and MO at 7.85 and 15.69 (w) has similar initial water content, the same water absorption were expected and, this result is consistent with the literature.

It is also described that the increased loads of polar drugs or adjuvants increase the water uptake of MO-based delivery systems, while the addition of nonpolar drugs decreases the water uptake (Chang and Bodmeier, 1997b; Kumar et al., 2004). In the present study, for both MO concentrations, the highest PEI concentration, which presents high cationic charge density at physiological pH due to its protonable amino group (Günther et al., 2011), promoted increase in the water absorption.

The swelling of the systems with and without PEI followed second order kinetics (Fig. 3B) according to Eq. (2). These results are consistent with other studies that have evaluated the MO water absorption profile (Lara et al., 2005; Rizwan et al., 2009; Souza et al., 2014). This demonstrated that in the beginning the percentage of swellable regions is high but after the swelling occurs, the ability to swell decreases due to two factors. First, the swelling rate is proportional to the amount of unrealized water uptake, which means that the increase in water absorption promotes an expansion and increases the stress on organized domains of the systems that resist more swelling. Second, the swelling rate is proportional to the area of the sites that have not interacted with water at time t, but will interact with water at a later time point (Schott, 1990).

Although *in vitro* swelling experiments will deviate from what occurs in biological fluids, these studies provide important insights

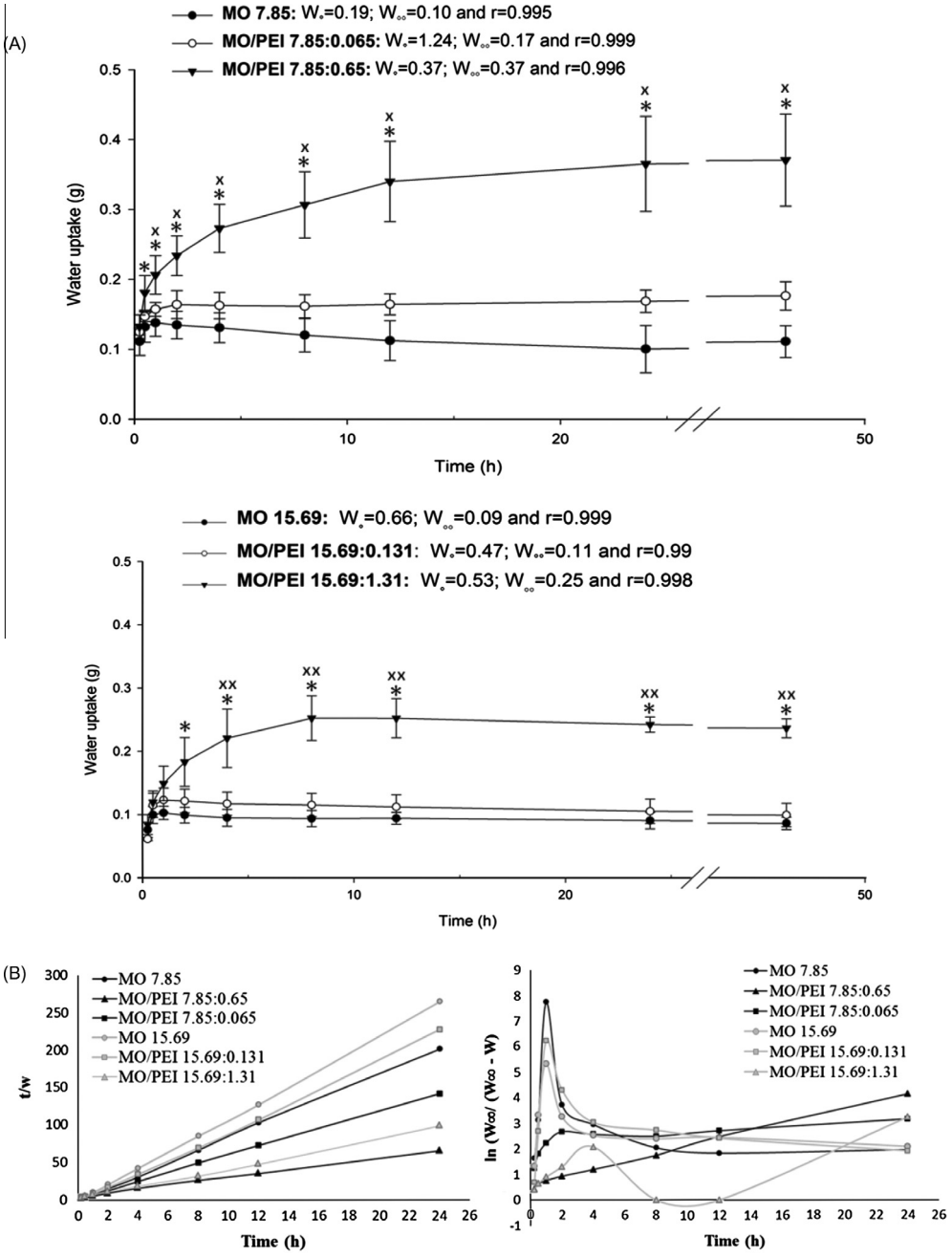

Fig. 3. (A) Plots of water uptake by the dialysis tubing with different formulations, expressed as a function of time. Statistical Analysis: one-way ANOVA ($n = 5$, ±E.P.M.). $^{*}p < 0.05$ compared to the formulation without PEI. $^{x}p < 0.05$ compared to the MO/PEI at 7.85:0.065 (w/w) and $^{xx}p < 0.05$ compared to the MO/PEI at 15.69:0.131 (w/w). Swelling kinetics parameters: W_o (initial rate of absorption; *g* water absorption/*g* formulation × hour); W_∞ (maximum water uptake; *g* water absorption/*g* formulation). (B) Swelling kinetics of different formulations with PEI and their controls, t/w versus time (second order kinetics) and ln $W_\infty/(W_\infty - W)$ versus time (first order kinetics). MO (monoglycerides), PEI (polyethylenimine). Temperature 37 °C.

into the kinetics of water uptake by the precursor fluid formulations and into how PEI interfered with LCS formation.

3.5. siRNA loading and its stability in precursor fluid formulations

Electrophoresis was performed to verify the ability of the developed MO/PEI-based systems to form complexes with siRNA. Fig. 4A shows that all of the MO/PEI-based formulations were able to form complexes with siRNA, even those with low concentrations of PEI. In contrast, control formulations, which lacked PEI, did not form complexes with siRNA. This study also showed that PEI had a better ability to complex siRNA than OAM, which at concentrations lower than 0.34% was not able to complex siRNA (Borgheti-Cardoso et al., 2014). Therefore, the presence of the PEI enabled the efficient incorporation of siRNA into the precursor fluid formulations.

After treatment with heparin, the complexed siRNA in the formulations was liberated in an intact form, as shown in Fig. 4B.

3.6. In vitro siRNA release from LC_2s

For the effective delivery of siRNA, it is essential that the siRNA is released in complex with PEI to avoid degradation and to facilitate its cellular uptake (Beyerle et al., 2011; Günther et al., 2011).

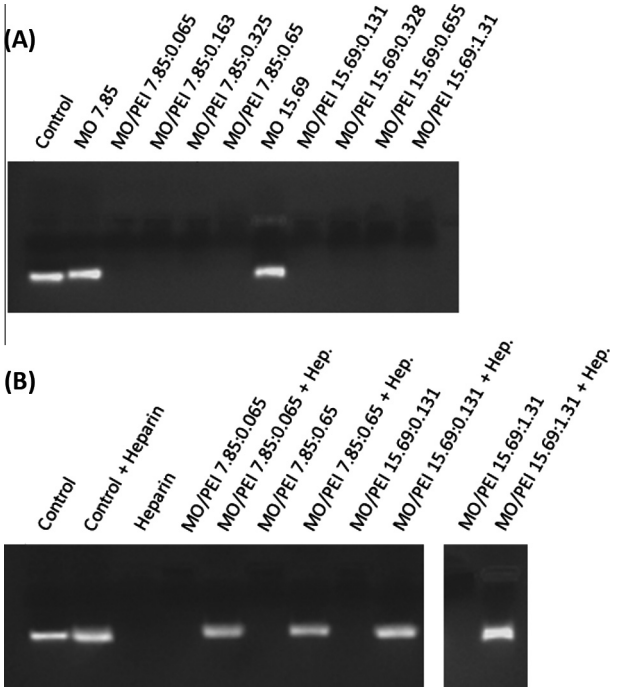

Fig. 4. (A) Loading efficiency of the precursor fluid formulations with different percentages of MO and PEI. (B) Evaluation of siRNA stability in different precursor fluid formulations using a heparin polyanion competition assay. Control: 10 μM siRNA in DEPC water. Hep: heparin, MO (monoglycerides), PEI (polyethylenimine).

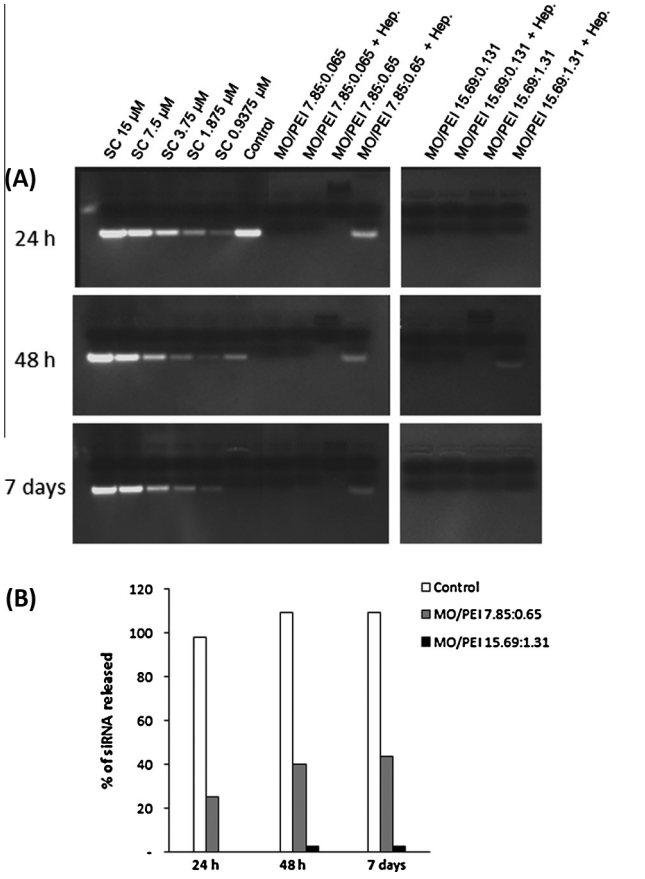

Fig. 5. (A) Release of siRNA from different formulations at 24, 48 h and 7 days as determined by qualitative analyses using agarose gel electrophoresis at 37 °C. (B) Release of siRNA from the control (white), inverted type liquid crystalline system obtained from the precursor formulations of MO/PEI/PG/Tris buffer at 7.85:0.65:76.5:15 (grey) and 15.69:1.31:68:15 (black) (w/w/w/w) analyzed by ImageJ. After 24 h, the % of siRNA released shown in the graph is cumulative. SC: standard curve. Control: siRNA in DEPC water (10 μM). MO (monoglycerides), PEI (polyethylenimine).

We used a heparin competition assay to determine whether the siRNA was released in the complexed form. Fig. 5A shows a qualitative evaluation by agarose gel electrophoresis of the siRNA released in the receptor medium from the precursor fluid formulations. The precursor fluid formulations composed of MO/PEI at 7.85:0.65 and 15.69:1.31 (w/w) released siRNA complexed with PEI because the siRNA was visualized only in the samples containing heparin.

Fig. 5B shows the percentage of siRNA released. As expected, the control (DEPC-treated water) released all of the siRNA (98% at 24 h, and reached 100% at 48 h). The LC_2 formed from the formulation composed of MO/PEI at 7.85:0.65 (w/w) released 25% of the siRNA at 24 h, which increased to 40% and 44% after 48 h and 7 days, respectively. The formulation composed of MO/PEI at 15.69:1.31 (w/w) released a mere 3% after 48 h. The LC_2s from the precursor fluid formulations composed of MO/PEI at 7.85:0.065 and 15.69:0.131 (w/w) did not release any siRNA during the analysis period.

In vitro drug release from LCSs has been investigated in several studies (Chang and Bodmeier, 1998; Lara et al., 2005; Phan et al., 2011; Rizwan et al., 2009); however, the release mechanism is still not completely understood. Several factors are involved and can influence the drug release including drug properties (which determine the solubilized drug concentration and its affinity for the water channel of the LCS), composition and structure of the LCSs (which are related to the initial water content, the water uptake rate and the size of the hydrophilic channels), and the experimental conditions used to perform the *in vitro* drug release (Yaghmur et al., 2013, 2012).

The influence of the initial water content on the drug release behavior was described previously and among the studies several conflicting results were found (Geraghty et al., 1996; Lara et al., 2005; Lee and Kellaway, 2000; Rizwan et al., 2009; Souza et al., 2014). Some of them reported that LCSs with higher initial water content allow a faster drug release because the matrices are better hydrated and have bigger hydrophilic water channels available for drug release (Chang and Bodmeier, 1997c; Lee and Kellaway, 2000). On the other hand, other authors demonstrated that there was no difference in the drug release behavior as a function of the initial water content because the water is rapidly taken up and the formation of a cubic phase occurs (Geraghty et al., 1996; Lara et al., 2005; Rizwan et al., 2009). In the present study, all the systems had similar water content (~15–16%), but showed different drug release rates. Thereby, for the studied systems, the initial water content seems not influence the drug release.

These differences in the release profile can be explained by the differences in water absorption. It has been reported that matrices that absorb more water can provide rapid diffusion and more rapid release than those with low water absorption. This is attributed to an increase in the channels available for release of hydrophilic drugs with increasing water content (Rizwan et al., 2009). In the present *in vitro* release study, the gel formed from the precursor fluid formulation composed of MO/PEI at 7.85:0.65 (w/w), which absorbed more water in the swelling studies, released its siRNA-PEI faster than the systems that absorbed less water.

The size of the channels of the LCSs was also used to explain the difference between the drug release rates of bicontinuous cubic and inverted hexagonal phases. It was reported that the release of hydrophilic drugs from inverted hexagonal phase is slower than from the bicontinuous cubic phase, probably due to the significant decrease in the size of hydrophilic channels of the hexagonal phase

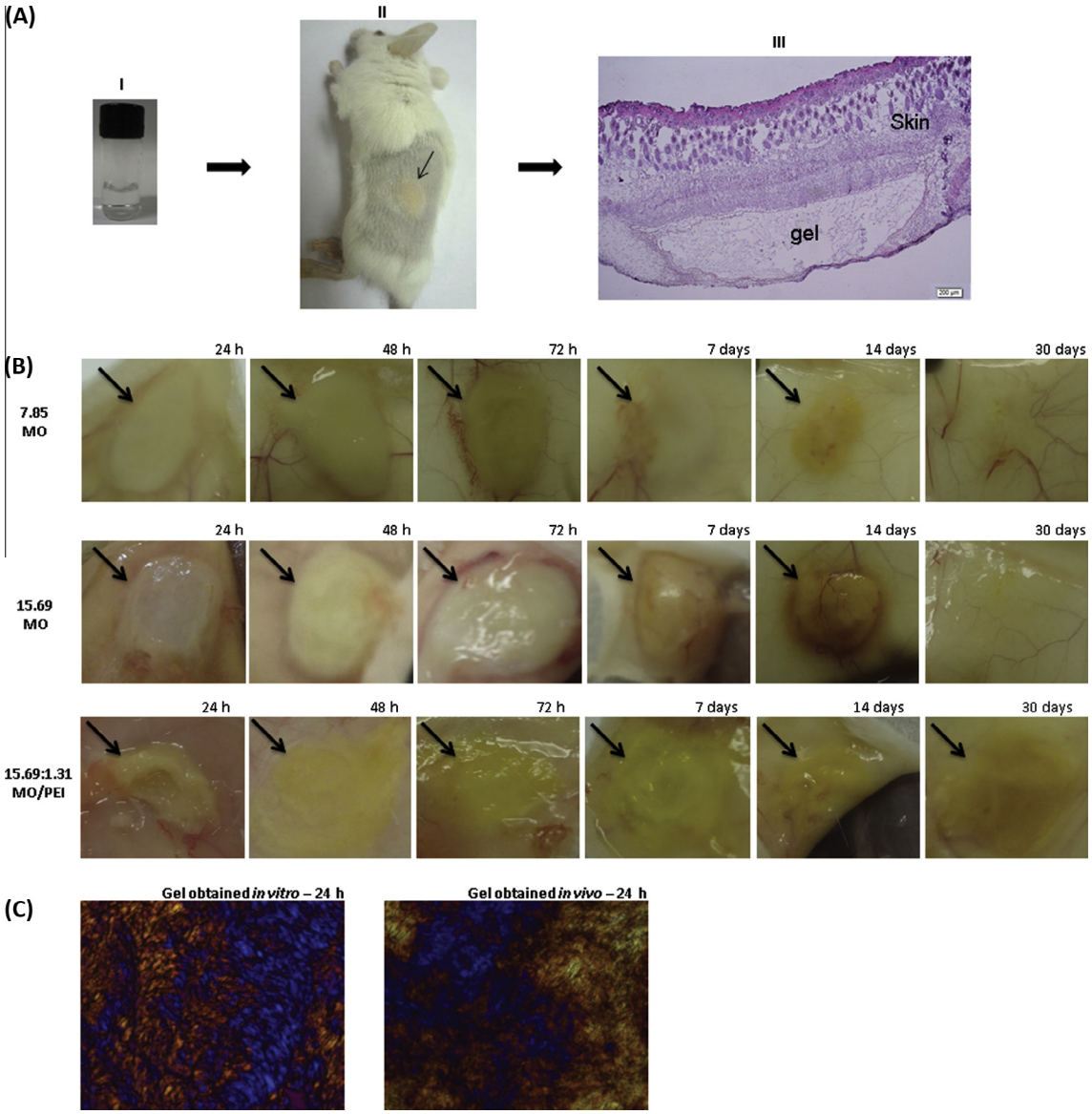

Fig. 6. (A) *In vivo* gel formation: (I) Precursor fluid formulation injected subcutaneously. (II) Localization of the gel *in vivo* in BALB/c mice. (III) H&E staining of skin with gel. (B) Gelling kinetics of systems with MO/PG/Tris buffer at 7.85:76.5:15.65 (w/w/w) and 15.69:68:16.31 (w/w/w) and MO/PEI/PG/Tris buffer 15.69:1.31:68:15 (w/w/w/w) administered subcutaneously in BALB/c mice at 24, 48 and 72 h and 7, 14 and 30 days. Gel formation is indicated by the arrow. The pictures were taken using macro mode without zooming, 10 cm from the subject (*f*-stop: *f*/2.6, exposure time: 1/250 s, exposure index: ISO-100). (C) Photomicrographs by polarized light microscopy of the system MO/PEI/PG/Tris buffer 15.69:1.31:68:15 (w/w/w/w) obtained 24 h from *in vitro* gelling formation assay and *in situ* gelling in animal model. Magnification 20×. Temperature 25 °C. MO (monoglycerides), PEI (polyethylenimine).

(Fong et al., 2009; Negrini and Mezzenga, 2011). Thereby, the release of hydrophilic drugs seems to be related to the diameter and the tortuosity of the water channels (Yaghmur et al., 2013), while the release of lipophilic drugs seems to depend on the localization of the solubilized drug molecules in the lipid–water interface or on the partitioning into the continuous hydrophobic domain (Yaghmur et al., 2013, 2012). Yaghmur et al. (2012) showed that the release of lipophilic drug from an inverted hexagonal phase does not lead to a slower drug release rate compared with bicontinuous cubic phase (Yaghmur et al., 2012). In the present study, the LC_2 formed from MO/PEI at 7.85:0.65 (w/w), characterized as a mixture of bicontinuous cubic phase with inverted hexagonal phase, showed higher siRNA release rates compared with MO/PEI at 7.85:0.065 (w/w), which was characterized as bicontinuous cubic phase. This result is in agreement with previous studies that showed that the diameter of water channel influences the drug release, because, as presented in Table 3, the LC_2 formed from MO/PEI at 7.85:0.65 (w/w) has a higher lattice parameter and probably a larger water channel than the LC_2 formed from the system MO/PEI at 7.85:0.065 (w/w).

3.7. In situ gel formation and biocompatibility study in mice

The subcutaneous injection of the precursor fluid formulations using a syringe and a 26 gauge needle was straightforward and well-tolerated in mice. To verify the influence of the amount of MO on *in situ* gel formation and local biocompatibility, precursor fluid formulations containing 7.85% and 15.69% MO without PEI were injected subcutaneously into the dorsal flank of mice. The *in situ* gelling process occurred upon injection. Fig. 6A shows a gel that formed *in vivo* and its subcutaneous location in a mouse. Fig. 6B shows the subcutaneous gels of both formulations and their degradation over several days. Gels obtained from the precursor fluid formulation containing 15.69% MO showed a larger volume

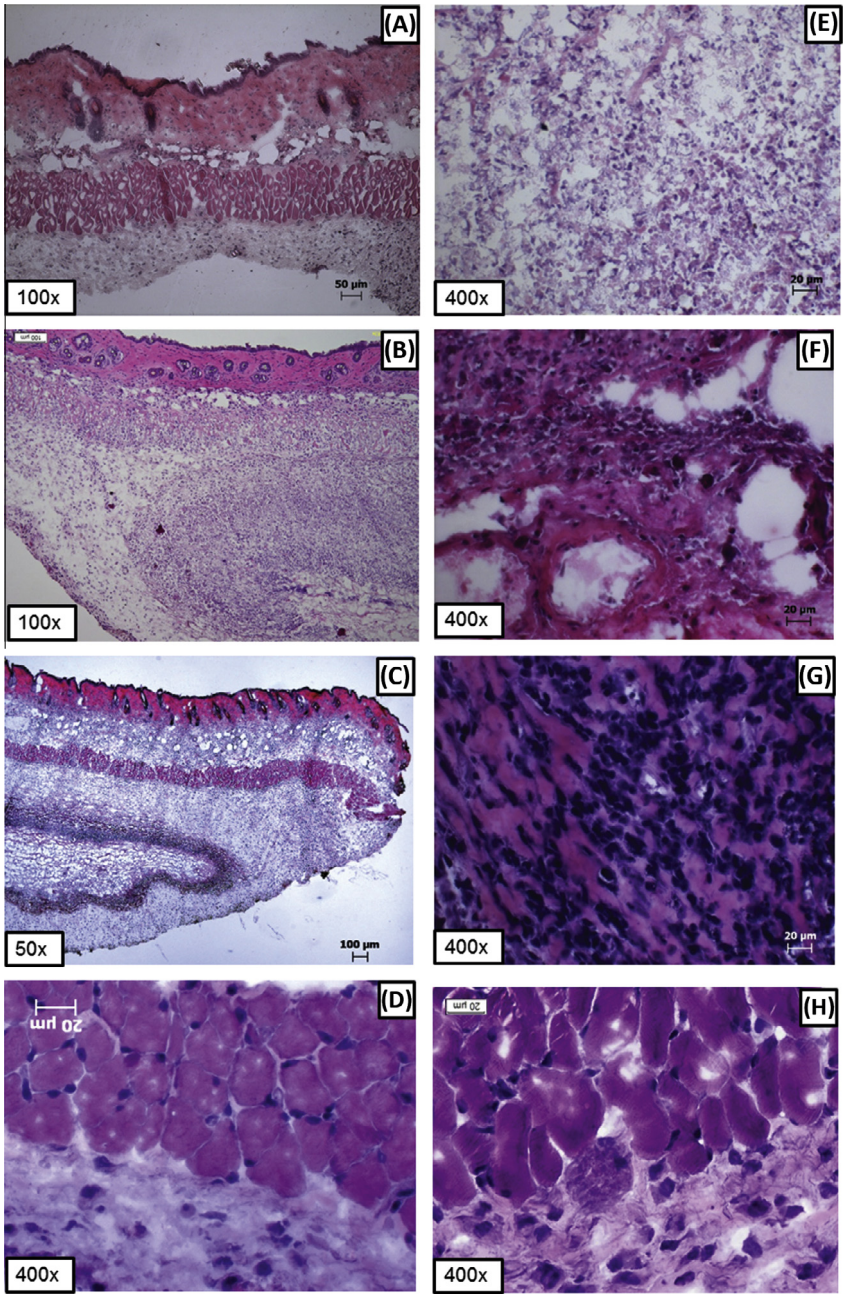

Fig. 7. Histological analysis of the slides stained with hematoxylin and eosin. (A, B and C) Skin and subcutaneous tissue 48 h after injection of saline, MO/PG/Tris buffer 7.85:76.5:15.65 (w/w/w) and MO/PG/Tris buffer 15.69:68:16.31 (w/w/w), respectively. (D) No inflammation was observed in subcutaneous tissue 48 h after administration of siRNA with saline (10 µM). (E) Degenerated cells around the gel with mononuclear infiltration 48 h after injection MO/PG/Tris buffer 7.85:76.5:15.65 (w/w/w). (F) Granulation tissue showing blood vessels, inflammatory cells and extracellular matrix 7 days after injection of MO/PEI/PG/Tris buffer 15.69:1.31:68:15 (w/w/w/w). (G) Fibroblasts and collagen fibers 14 days after injection of MO/PG/Tris buffer 7.85:76.5:15.65 (w/w/w). (H) Injury repair (Fibroblasts and collagen fibers) 30 days after administration of MO/PG/Tris buffer 15.69:68:16.31 (w/w/w). MO (monoglycerides), PEI (polyethylenimine), PG (propylene glycol).

than the gel formed by the formulation containing 7.85% MO. Both gels formed from 7.85% and 15.69% MO maintained their integrity for at least 14 days. By 30 days, no gel residue was observed in the subcutaneous tissue for both formulations. The degradation of the gels likely occurs by lipolysis caused by different types of esterases that are present in tissues (Shah et al., 2001). The hydrolysis of MO into glycerol and oleic acid is a slow process that can be accelerated by lipases (Caboi et al., 2001). Moreover, the process can be affected by various factors such as pH, composition of the surrounding biological fluid, light and/or temperature. The system containing the highest PEI concentration (MO/PEI at 15.69:1.31 (w/w)) showed the same gel formation as the systems without PEI, but the degradation was slower given that traces of gel were still observed in the subcutaneous tissue in 30 days (Fig. 6B). This result suggests that PEI may play a role in maintaining the gel at the site of application. Samples of this gel formed in the subcutaneous tissue were collected and were found to be in the hexagonal phase under a polarized light microscope (Fig. 6C). This result demonstrated that the gels that form both *in vivo* and *in vitro* are in the same liquid crystalline phase as identified by polarized light microscopy (Table 1).

Local toxicity is a concern for subcutaneous injection (Dreischalück et al., 2010). Therefore, the local tissue response was evaluated by histology, using H&E, of excised samples of skin

and gel with sufficient surrounding tissue for up to 30 days after subcutaneous administration. Saline with and without siRNA (10 μm) were injected as controls. In these mice, no inflammation was observed (Fig. 7A and D). As shown in Fig. 7, precursor fluid formulations containing 7.85% and 15.69% MO without PEI and MO/PEI at 15.69:1.31 (w/w) perturbed neither dermal nor epidermal characteristics after subcutaneous injections. However, tissues directly around the gel responded by recruiting inflammatory cells. Twenty-four hours after subcutaneous administration, the presence of polymorphonuclear cells was observed. After 48 h, a predominance of mononuclear cells, such as macrophages, was observed and after 7 days, granulation tissue showing blood vessels, inflammatory cells and extracellular matrix was seen for all LCS formulations. After 14 days, fibroblasts and collagen fibers were observed in the tissue around the gels formed from the precursor fluid formulations of 7.85% MO, suggesting the presence of ongoing tissue repair. At higher concentrations of MO (15.69%) the tissue repair process lasted for 30 days. In the presence of PEI (MO/PEI at 15.69:1.31 (w/w)), fibroblasts and collagen fibers were not observed during the analysis period.

This biocompatibility study indicated that MO was the component that caused tissue response, because 7.85% MO resulted in faster tissue repair and less inflammatory cell recruitment than 15.69% MO. PEI, a component with irritating properties, appeared to have little additional influence on the tissue because the systems with and without PEI had similar effects. The absence of PEI-mediated consequences may be due to its internal localization in the liquid crystalline phase of the formed gel. This effect of MO is intriguing because MO alone is considered nontoxic (Kulkarni et al., 2011). A possible explanation is that the volume of the *in situ* formed gel exerted pressure on the surrounding tissue by absorbing water, thereby physically rather than chemically damaging tissue leading to the recruitment of inflammatory cells. Similar observations were made on a Poloxamer 407 gel, where physical presence of the gel caused mechanical irritation (Ricci et al., 2005). The inflammatory process promoted by gel formation in the system containing 7.85% MO was self-limiting and the tissue normalized after a few days. In addition, the animals behaved normally, further supporting that the inflammatory response was limited. Therefore, systems containing 7.85% MO may be appropriate for subcutaneous delivery because the inflammation was mild and the tissue regenerated.

The systems developed in this study may represent a new approach to the local delivery of molecules such as siRNA because they act as a depot that can protect the siRNA against degradation and can control its release. Additionally, these systems are minimally invasive and are biodegradable.

4. Conclusions

The present study demonstrates that the proper combination of MO, PEI, PG and Tris buffer can form an *in situ* gelling delivery system for local siRNA release. The addition and concentration of PEI into LCSs influences the phase behavior, water absorption and drug release profile of the LC_2. Moreover, the presence of PEI is essential to complex siRNA.

The system composed by MO/PEI/PG/Tris buffer at 7.85:0.65:76.5:15 (w/w/w/w), characterized as bicontinuous cubic phase with an interstice of inverted hexagonal phase (after contact with excess water), appears to be the best system for the local delivery of siRNA. After addition of siRNA the system was characterized as a mixture of bicontinuous cubic phase and inverted hexagonal phase. The LC_2 formation of this formulation is rapid, and the siRNA is released as a complex with PEI, which is necessary for the effectiveness of the proposed systems as nucleic acid carriers. Additionally, the gel formed *in situ* after subcutaneous injection is biodegradable and presents low local toxicity.

Therefore, the *in situ* gelling system developed is a potential delivery system for local administration of siRNA. Further studies will be performed to verify gene silencing efficiencies.

Acknowledgments

The authors thank Emerson de Souza Santos for teaching them how to use ImageJ. This study was supported by São Paulo Research Foundation (FAPESP, Brazil) Grant #04/09465-7, and by "Conselho Nacional de Desenvolvimento Científico e Tecnológico" (CNPq, Brazil). L.N. Borgheti-Cardoso was the recipient of a CNPq fellowship (grant # 134780/2010-8) and FAPESP fellowship (Grants # 2010/11736-0 and # 2013/02132-1).

References

Agarwal, P., Rupenthal, I.D., 2013. Injectable implants for the sustained release of protein and peptide drugs. Drug Discov. Today 18, 337–349.
Amar-Yuli, I., Garti, N., 2005. Transitions induced by solubilized fat into reverse hexagonal mesophases. Colloids Surface B Biointerface 43, 72–82.
Amar-Yuli, I., Wachtel, E., Shoshan, E.B., Danino, D., Aserin, A., Garti, N., 2007. Hexosome and hexagonal phases mediated by hydration and polymeric stabilizer. Langmuir 23, 3637–3645.
Amar-Yuli, I., Aserin, A., Garti, N., 2008. Solubilization of nutraceuticals into reverse hexagonal mesophases. J. Phys. Chem. B 112, 10171–10180.
Aota-Nakano, Y., Jie, S., Yamazaki, M., 1999. Effects of electrostatic interaction on the phase stability and structures of cubic phases of monoolein/oleic acid mixture membranes. Biochim. Biophys. Acta 1461, 96–102.
Beyerle, A., Braun, A., Merkel, O., Koch, F., Kissel, T., Stoeger, T., 2011. Comparative in vivo study of poly(ethylene imine)/siRNA complexes for pulmonary delivery in mice. J. Control. Release 151, 51–56.
Borgheti-Cardoso, L.N., Depieri, L.V., Diniz, H., Calzzani, R.A.J., De Abreu Fantini, M.C., Iyomasa, M.M., De Carvalho, Moura., Vicentini, F.T., Bentley, M.V.L.B., 2014. Self-assembling gelling formulation based on a crystalline-phase liquid as a non-viral vector for siRNA delivery. Eur. J. Pharm. Sci. 58, 72–82.
Caboi, F., Amico, G.S., Pitzalis, P., Monduzzi, M., Nylander, T., 2001. Addition of hydrophilic and lipophilic compounds of biological relevance to the monoolein/water system. I. Phase behavior. Chem. Phys. Lipids 109, 47–62.
Chang, C.M., Bodmeier, R., 1997a. Binding of drugs to monoglyceride-based drug delivery systems. Int. J. Pharm. 147, 135–142.
Chang, C.M., Bodmeier, R., 1997b. Swelling of and drug release from monoglyceride-based drug delivery systems. J. Pharm. Sci. 86, 747–752.
Chang, C.M., Bodmeier, R., 1997c. Effect of dissolution media and additives on the drug release from cubic phase delivery systems. J. Control. Release 46, 215–222.
Chang, C.M., Bodmeier, R., 1998. Low viscosity monoglyceride-based drug delivery systems transforming into a highly viscous cubic phase. Int. J. Pharm. 173, 51–60.
Clogston, J., Rathman, J., Tomasko, D., Walker, H., Caffrey, M., 2000. Phase behavior of a monoacylglycerol (Myverol 18–99K):water system. Chem. Phys. Lipids 107, 191–220.
De Campo, L., Yaghmur, A., Sagalowicz, L., Leser, M.E., Watzke, H., Glatter, O., 2004. Reversible phase transitions in emulsified nanostructured lipid systems. Langmuir 20, 5254–5261.
Dreischalück, J., Schwöppe, C., Spieker, T., Kessler, T., Tiemann, K., Liersch, R., Schliemann, C., Kreuter, M., Kolkmeyer, A., Hintelmann, H., Mesters, R.M., Berdel, W.E., Dreischaluck, J., Schwoppe, C., 2010. Vascular infarction by subcutaneous application of tissue factor targeted to tumor vessels with NGR-peptides: activity and toxicity profile. Int. J. Oncol. 37, 1389–1397.
Engelskirchen, S., Maurer, R., Glatter, O., 2011. Effect of glycerol addition on the internal structure and thermal stability of hexosomes prepared from phytantriol. Colloids Surf. A Physicochem. Eng. Asp. 391, 95–100.
Engstrom, S., Engstrom, L., 1992. Phase behaviour of the lidocaine-monoolein-water system. Int. J. Pharm. 79, 113–122.
Fire, A., Xu, S., Montgomery, M.K., Kostas, S.A., Driver, S.E., Mello, C.C., 1998. Potent and specific genetic interference by double-stranded RNA in *Caenorhabditis elegans*. Nature 391, 806–811.
Fong, W.K., Hanley, T., Boyd, B.J., 2009. Stimuli responsive liquid crystals provide "on-demand" drug delivery *in vitro* and in vivo. J. Control. Release 135, 218–226.
Fong, C., Le, T., Drummond, C.J., 2012. Lyotropic liquid crystal engineering-ordered nanostructured small molecule amphiphile self-assembly materials by design. Chem. Soc. Rev. 41, 1297.
Geraghty, P.B., Attwood, D., Collett, J.H., Dandiker, Y., 1996. The *in vitro* release of some antimuscarinic drugs from monoolein/water lyotropic liquid crystalline gels. Pharm. Res. 13, 1265–1271.
Günther, M., Lipka, J., Malek, A., Gutsch, D., Kreyling, W., Aigner, A., Gunther, M., 2011. Polyethylenimines for RNAi-mediated gene targeting in vivo and siRNA delivery to the lung. Eur. J. Pharm. Biopharm. 77, 438–449.

Guzman-Villanueva, D., El-Sherbiny, I.M., Herrera-Ruiz, D., Vlassov, A.V., Smyth, H.D.C., 2012. Formulation approaches to short interfering RNA and MicroRNA: challenges and implications. J. Pharm. Sci. 101, 4046–4066.
Han, K., Pan, X., Chen, M., Wang, R., Xu, Y., Feng, M., Li, G., Huang, M., Wu, C., 2010. Phytantriol-based inverted type bicontinuous cubic phase for vascular embolization and drug sustained release. Eur. J. Pharm. Sci. 41, 692–699.
Han, H.D., Mora, E.M., Roh, J.W., Nishimura, M., Lee, S.J., Stone, R.L., Bar-Eli, M., Lopez-Berestein, G., Sood, A.K., 2011. Chitosan hydrogel for localized gene silencing. Cancer Biol. Ther. 11, 839–845.
Hatefi, A., Amsden, B., 2002. Biodegradable injectable *in situ* forming drug delivery systems. J. Control. Release 80, 9–28.
Kim, Y.M., Park, M.R., Song, S.C., 2012. Injectable polyplex hydrogel for localized and long-term delivery of siRNA. ACS Nano 6, 5757–5766.
Krebs, M.D., Jeon, O., Alsberg, E., 2009. Localized and sustained delivery of silencing RNA from macroscopic biopolymer hydrogels. J. Am. Chem. Soc. 131, 9204–9206.
Kulkarni, C.V., Wachter, W., Iglesias-Salto, G., Engelskirchen, S., Ahualli, S., 2011. Monoolein: a magic lipid? Phys. Chem. Chem. Phys. 13, 3004–3021.
Kumar, M.K., Shah, M.H., Ketkar, A., Mahadik, K.R., Paradkar, A., 2004. Effect of drug solubility and different excipients on floating behaviour and release from glyceryl monooleate matrices. Int. J. Pharm. 272, 151–160.
Landh, T., 1994. Phase-behavior in the system pine oil monoglycerides-poloxamer-407-water at 20-degrees-C. J. Phys. Chem. 98, 8453–8467.
Lara, M.G., Bentley, M.V., Collett, J.H., 2005. *In vitro* drug release mechanism and drug loading studies of cubic phase gels. Int. J. Pharm. 293, 241–250.
Larsson, K., 1989. Cubic lipid–water phases: structures and biomembrane aspects. J. Phys. Chem. 93, 7304–7314.
Lee, J., Kellaway, I.W., 2000. Buccal permeation of [D-Ala(2), D-Leu(5)]enkephalin from liquid crystalline phases of glyceryl monooleate. Int. J. Pharm. 195, 35–38.
Li, Z., Ning, W., Wang, J., Choi, A., Lee, P.Y., Tyagi, P., Huang, L., 2003. Controlled gene delivery system based on thermosensitive biodegradable hydrogel. Pharm. Res. 20, 884–888.
Libster, D., Aserin, A., Wachtel, E., Shoham, G., Garti, N., 2007. An HII liquid crystal-based delivery system for cyclosporin A: physical characterization. J. Colloid Interface Sci. 308, 514–524.
Lindblom, G., Rilfors, L., 1989. Cubic phase and isotropic structures formed by membrane lipids-possible biological relevance. Biochim. Biophys. Acta 988, 221–256.
Liu, Z., Zheng, M., Meng, F., Zhong, Z., 2011. Non-viral gene transfection *in vitro* using endosomal pH-sensitive reversibly hydrophobilized polyethylenimine. Biomaterials 32, 9109–9119.
Liu, Q., Dong, Y.D., Hanley, T.L., Boyd, B.J., 2013. Sensitivity of nanostructure in charged cubosomes to phase changes triggered by ionic species in solution. Langmuir 29, 14265–14273.
Mezzenga, R., Grigorov, M., Zhang, Z.D., Servais, C., Sagalowicz, L., Romoscanu, A.I., Khanna, V., Meyer, C., 2005. Polysaccharide-induced order-to-order transitions in lyotropic liquid crystals. Langmuir 21, 6165–6169.
Milak, S., Zimmer, A., 2015. Glycerol monooleate liquid crystalline phases used in drug delivery systems. Int. J. Pharm. 478, 569–587.
Mitchell, D.J., Ninham, B.W., 1981. Micelles, vesicles and micro-emulsions. J. Chem. Soc. Trans. 77, 601–629.
Negrini, R., Mezzenga, R., 2011. PH-responsive lyotropic liquid crystals for controlled drug delivery. Langmuir 27, 5296–5303.
Nguyen, K., Dang, P.N., Alsberg, E., 2013. Functionalized, biodegradable hydrogels for control over sustained and localized siRNA delivery to incorporated and surrounding cells. Acta Biomater. 9, 4487–4495.
Packhaeuser, C.B., Schnieders, J., Oster, C.G., Kissel, T., 2004. *In situ* forming parenteral drug delivery systems: an overview. Eur. J. Pharm. Biopharm. 58, 445–455.
Peer, D., Lieberman, J., 2011. Special delivery: targeted therapy with small RNAs. Gene Ther. 18, 1127–1133.
Persson, G., Edlund, H., Lindblom, G., 2003. Thermal behaviour of cubic phases rich in 1-monooleoyl-rac-glycerol in the ternary system: 1-monooleoyl-rac-glycerol/n-octyl-β-d-glucoside/water. Eur. J. Biochem. 270, 56–65.
Phan, S., Fong, W.K., Kirby, N., Hanley, T., Boyd, B.J., 2011. Evaluating the link between self-assembled mesophase structure and drug release. Int. J. Pharm. 421, 176–182.
Qiu, H., Caffrey, M., 2000. The phase diagram of the monoolein/water system: metastability and equilibrium aspects. Biomaterials 21, 223–234.
Ricci, E.J., Lunardi, L.O., Nanclares, D.M., Marchetti, J.M., 2005. Sustained release of lidocaine from Poloxamer 407 gels. Int. J. Pharm. 288, 235–244.
Rizwan, S.B., Hanley, T., Boyd, B.J., Rades, T., Hook, S., 2009. Liquid crystalline systems of phytantriol and glyceryl monooleate containing a hydrophilic protein: characterisation, swelling and release kinetics. J. Pharm. Sci. 98, 4191–4204.
Rossetti, F.C., Fantini, M.C., Carollo, A.R., Tedesco, A.C., Bentley, M.V., 2011. Analysis of liquid crystalline nanoparticles by small angle X-ray diffraction: evaluation of drug and pharmaceutical additives influence on the internal structure. J. Pharm. Sci. 100, 2849–2857.
Schott, H., 1990. Kinetics of swelling of polymers and their gels. J. Pharm. Sci. 81, 467–470.
Shah, J.C., Sadhale, Y., Chilukuri, D.M., 2001. Cubic phase gels as drug delivery systems. Adv. Drug Deliv. Rev. 47, 229–250.
Shen, Y., Wang, B., Lu, Y., Ouahab, A., Li, Q., Tu, J., 2011. A novel tumor-targeted delivery system with hydrophobized hyaluronic acid-spermine conjugates (HHSCs) for efficient receptor-mediated siRNA delivery. Int. J. Pharm. 414, 233–243.
Souza, C., Watanabe, E., Borgheti-Cardoso, L.N., Fantini, M.C., Lara, M.G., 2014. Mucoadhesive system formed by liquid crystals for buccal administration of PHMB. J. Pharm. Sci. 103, 3914–3923.
Tran, M.A., Gowda, R., Sharma, A., Park, E.-J., Adair, J., Kester, M., Smith, N.B., Robertson, G.P., 2008. Targeting V600EB-Raf and Akt3 using nanoliposomal-small interfering RNA inhibits cutaneous melanocytic lesion development. Cancer Res. 68, 7638–7649.
Vicentini, F.T.M.D.C., Borgheti-cardoso, L.N., Depieri, L.V., De MacEdo Mano, D., Abelha, T.F., Petrilli, R., Bentley, M.V.L.B., Macedo, D..De., 2013. Delivery systems and local administration routes for therapeutic siRNA. Pharm. Res. 30, 915–931.
Wong, S.Y., Pelet, J.M., Putnam, D., 2007. Polymer systems for gene delivery-past, present, and future. Prog. Polym. Sci. 32, 799–837.
Yaghmur, A., Laggner, P., Zhang, S., Rappolt, M., 2007. Tuning curvature and stability of monoolein bilayers by designer lipid-like peptide surfactants. PLoS ONE 2 (5), e479.
Yaghmur, A., Larsen, S.W., Schmitt, M., Østergaard, J., Larsen, C., Jensen, H., Urtti, A., Rappolt, M., 2011. *In situ* characterization of lipidic bupivacaine-loaded formulations. Soft Matter 7, 8291.
Yaghmur, A., Rappolt, M., Oøstergaard, J., Larsen, C., Larsen, S.W., 2012. Characterization of bupivacaine-loaded formulations based on liquid crystalline phases and microemulsions: the effect of lipid composition. Langmuir 28, 2881–2889.
Yaghmur, a., Rappolt, M., Larsen, S.W., 2013. *In situ* forming drug delivery systems based on lyotropic liquid crystalline phases: structural characterization and release properties. J. Drug Deliv. Sci. Technol. 23, 325–332.
Yin, H., Kanasty, R.L., Eltoukhy, A.A., Vegas, A.J., Dorkin, J.R., Anderson, D.G., 2014. Non-viral vectors for gene-based therapy. Nat. Rev. Genet. 15, 541–555.
Zabara, A., Amar-yuli, I., Mezzenga, R., 2011. Tuning in-meso-crystallized lysozyme polymorphism by lyotropic liquid crystal symmetry. Langmuir 27, 6418–6425.
Zheng, L., Zhang, J., Shui, L., Chen, F., Um, J., Chung, H., 2003. Component effects on the phase behavior of monoglyceride–water mixtures studied by FT-IR and X-ray diffraction. J. Dispers. Sci. Technol. 24, 773–778.